Available online at www.sciencedirect.com
SCIENCE DIRECT®
Journal of Power Sources 128 (2004) 1–12
JOURNAL OF POWER SOURCES
www.elsevier.com/locate/jpowsour

Characteristics of a direct methanol fuel cell based on a novel electrode assembly using microporous polymer membranes

R.W. Reeve[1], G.T. Burstein*, K.R. Williams

Department of Materials Science and Metallurgy, University of Cambridge, Pembroke Street, Cambridge CB2 3QZ, UK

Received 29 April 2003; received in revised form 8 July 2003; accepted 28 July 2003

Abstract

This paper describes work carried out on novel electrode assemblies based on the use of microporous plastics for application in a direct methanol fuel cell. The results are compared with those from similar assemblies based on carbon paper. Studies of the oxygen reduction reaction for a platinum electrode carrying 0.88 mg Pt/cm^2 on a spun-bonded polyethylene substrate gave a current density of 280 mA/cm^2 at 0.64 V(SHE) at 75 °C (uncorrected for the ohmic potential drop). The platinum utilisation of this electrode system was found to increase with decreasing loading with the lowest loading of 0.08 mg Pt/cm^2 giving almost 1.2 A/mg Pt at the same potential. Methanol electrodes based on these same membranes gave 266 mA/cm^2 for a loading of 0.95 mg Pt + Ru (60:40) at 0.64 V(SHE) (uncorrected for the ohmic potential drop) running on methanol vapour at 75 °C. Again, decreasing the loading increased the catalyst utilisation with a 0.18 mg Pt + Ru (60:40) electrode giving over 1 A/mg Pt. Carbon paper-based electrodes showed the best overall performance toward methanol oxidation. However, these electrodes were found difficult to control both in half-cell and single-cell experiments because of leakage of the electrolyte. A single cell employing a circulating sulphuric acid electrolyte was used to evaluate the various electrode systems. In general, the cell output followed the behaviour predicted from the results of the half cells. Outputs ranged from 10 to 32 W/g Pt and from 5 to 15 mW/cm^2 at 75 °C, depending upon the electrode system. The cell outputs were limited partly by the high resistance of the electrolyte which occurred as a result of the high interelectrode gap used for these experiments.

Keywords: Fuel cell; DMFC; Direct methanol fuel cell; Methanol anode; Air cathode; Oxygen cathode

1. Introduction

The direct methanol fuel cell (DMFC) offers a potential replacement for the internal combustion engine in motor vehicle applications, as well as having possible uses in many other areas. A stack of such cells is in principle capable of powering an electrically driven vehicle, either alone or coupled with secondary batteries in hybrid configuration. Such a power system should be far cleaner in terms of emissions, allow greater efficiency of use of carbonaceous fuels, and it is quieter than combustion power units. Such a system could also in some ways be safer than a hydrogen-powered fuel cell system: carriage of hydrogen in any form on board is potentially hazardous, particularly in the event of an accident. On-board generation of hydrogen requires high temperatures and associated reduced efficiency, as well as correspondingly high cost. One alternative to the hydrogen energy source in fuel cells is the direct methanol fuel cell, but much development, both scientific and technological, is required before the DMFC systems can be usefully put into practice.

To date, there are essentially two types of DMFCs: those which use sulphuric acid as electrolyte and those which use proton conducting polymer membranes, such as those based on perfluorosulphonic acid (e.g. Nafion), or H_3PO_4-doped polybenzamidazole. The latter have recently been shown to be able to develop very high power outputs, e.g. 200–400 mW/cm^2 [1–3]. This is due to a combination of the low ohmic resistance of the very thin membranes used (typically 110–120 μm) together with the extremes of temperature and pressures used (typically 100–200 °C and 3–5 bar) in these studies. Although these outputs appear promising, the extra cost together with the overall system efficiency loss as a result of having to compress the fuel and oxidant may limit their application. Another drawback of such cells is the high cost of the membrane itself together with the cost of the machined graphite separator plates or

* Corresponding author. Tel.: +44-1223-334-361; fax: +44-1223-334-567.
E-mail address: gtb1000@cus.cam.ac.uk (G.T. Burstein).
[1] Present address: Qinetiq Ltd., Haslar Marine Technology Park, Gosport, Hants PO12 2AG, UK.

0378-7753/$ – see front matter © 2003 Elsevier B.V. All rights reserved.
doi:10.1016/j.jpowsour.2003.07.006

current collector end plates which are used in these cells. In addition, methanol cross-over to the cathode has been identified as a major performance loss mechanism in cells based on solid polymer electrolytes [4–9].

The purpose of this paper is to present the results of work carried out using a low-cost electrolyte system incorporating sulphuric acid and microporous membranes for use in the DMFC. The membrane electrode assembly consists of electrode substrates, particularly those made from low-cost microporous polymer sheet, which were coated with electrocatalyst on one side, and impregnated with sulphuric acid solution. We showed earlier [10] that a membrane employing a glass microfibre mat infiltrated with sulphuric acid could be used as an unpressurised hydrogen anode with effective performance. Apart from its low cost, sulphuric acid solutions also have a very high ion conductivity (a maximum at 25 °C of 0.74 S/cm at a concentration of 3.7 M [11]).

2. Experimental

2.1. Electrode/substrate preparation

Electrodes were prepared by application of a catalyst layer to various microporous substrates. Details of the microporous substrates are given below. Apart from the carbon paper, the microporous substrates were commercially available sheet polymers. To create electrical conductivity for the electrode assembly, the microporous polymer substrates were plated with gold on one side, the side which would also carry the electrocatalyst. Electron conduction could thereby occur from the catalyst particles via the gold layer to the external circuit. Gold plating was done by first applying a thin layer of gold using thermal evaporation. This thin layer was then thickened up to ca. 1 μm by electrodeposition from a cyanide-free BDT gold bath (Enthone-OMI (UK) Ltd.). Prior to the first application by thermal evaporation, the substrates were subjected to bombardment by a beam of argon ions in a vacuum chamber to render the surfaces clean.

In the course of this work, both carbon-supported and unsupported platinum-based catalysts were used. Supported catalysts in the form of Pt on carbon were supplied by Johnson-Matthey plc. Alternatively, platinum black (Aldrich) and Adams platinum/ruthenium catalysts were used. The Adams Pt/Ru was prepared by dissolving stoichiometric amounts of $RuCl_3$ (Aldrich), hexachloroplatinic acid (H_2PtCl_6 supplied by Johnson-Matthey plc.) and sodium nitrate (a.r. grade) in twice-distilled water. After thorough mixing, the water was boiled off under application of heat, and the residue was allowed to melt by further heating, before being poured directly into twice-distilled water. The resulting suspension was then allowed to settle and the excess water with dissolved sodium nitrate decanted off. The solids were then suspended again in twice-distilled water, and again left to settle before being collected on a watch glass and dried slowly in an oven at 80 °C. The resulting Adams Pt/Ru catalyst was thus formed without carbon support.

The catalyst powders were applied to the substrates in the form of an “ink”, made by suspending the catalyst with a binder in a solvent. The compositions of the electrodes produced varied according to the catalyst powder used and the ink composition; these are given in Table 1. Note that Table 1 employs identification numbers for the different inks which are referred to in presentation of the experimental results. Nafion (5 wt.% solution, Aldrich) was used as the catalyst binder and analytical grade ethandiol (Fisher Scientific) used as a high-temperature solvent, together with water. In general, between 0.1 and 0.2 g of the catalyst or supported catalyst was mixed with approximately 1.5 cm^3 ethandiol, 0.5 cm^3 water and 1 cm^3 solublised Nafion solution (5 wt.%). When making up the ink, the catalyst was always wetted with water first in order to prevent excessive reaction with the Nafion solution. The ink mixture was then mixed thoroughly and subjected to ultrasonic treatment for 30 min for effective dispersion.

The catalyst was applied to the substrate in layers. These were built up to the required loading by repeated application of the ink, either by painting or spraying, followed by drying in an oven at 80 °C. The electrodes were then placed in a die to retain their shape and heated to 120 °C for 45–60 min in order for the Nafion to bind the catalyst particles together. In the case of the Adams platinum/ruthenium catalysts and the platinum black catalysts, it was found necessary to add a small amount of the corresponding supported catalyst (carbon-supported) to the ink in order for the electrode to bind adequately.

Prior to testing in the electrochemical cell, the electrodes were infiltrated with electrolyte under vacuum in a desiccator for 10 min. In the case of the Adams Pt/Ru electrodes,

Table 1
Compositions of the catalyst inks

Ink no. and type	Pt (wt.%)	Ru (wt.%)	C (wt.%)	Nafion (wt.%)	PTFE (wt.%)
Ink 1: JM carbon-supported Pt	15	–	60	25	–
Ink 2: JM carbon-supported Pt/Ru	15	7	53	25	–
Ink 3: JM carbon-supported Pt + platinum black mix	55	–	20	25	–
Ink 4: JM carbon-supported Pt/Ru + Adams Pt/Ru (no. 1)	21	14	43	22	–
Ink 5: JM carbon-supported Pt/Ru + Adams Pt/Ru (no. 2)	30	26	18	26	–
Ink 6: JM carbon-supported Pt + PTFE	14	–	54	23	9

JM indicates Johnson-Matthey Pt or Pt/Ru, both supported on carbon.

it was useful to provide a reduction treatment prior to use, either by reduction under hydrogen or by polarisation at −0.7 V (versus the mercury/mercurous sulphate (MMS) reference electrode) in deaerated 1.5 M sulphuric acid. Hydrogen evolution was also used as a conditioning stage for some half-cell test electrodes; this procedure as a treatment prior to use was found to increase the current output significantly. The improved performance generated by prior cathodic hydrogen treatment in this fashion may be due to the expulsion of organic residues from the electrode pores (produced from ethandiol and Nafion solutes) or perhaps to the reduction of residual surface oxides, particularly those of Ru. The working electrolyte used in the cell, and also infiltrated into the microporous polymers was sulphuric acid, of concentration either 1.5 or 3 M, made from analytical grade reagent and twice-distilled water. All water used throughout the entire research programme, for synthesis, electrode preparation, electrolytes, cleaning, etc. had been distilled twice prior to use.

2.2. Half-cell and single-cell testing

The method used to test electrodes is similar to that described earlier [12–15]. The performance of individual electrodes was measured in a half-cell arrangement built using a modular design. Each part was machined from polytetrafluoroethylene (PTFE) to provide an electrochemical cell of internal cylindrical symmetry whose diameter was the same as that of the working electrode. With the exception of the methanol and oxygen/air feed systems, the equipment and construction were the same for both anode and cathode studies. The electrolyte, either 1.5 or 3 M H_2SO_4 (always analytical grade), was circulated and heated via a gas-lift circulator mounted external to the cell. This home-built gas-lift pump, which was also used to deaerate the working electrolyte, employed argon as a drive to draw electrolyte from the cell through a Pyrex glass loop which also carried a small home-built wire-wound heating jacket. The deaerating argon forced the electrolyte through the heated section via a small loop back to the working cell. The heater was controlled by a thermistor mounted inside the cell remote from the working electrode.

The counter electrode was a sheet of Pt foil (Johnson-Matthey plc.) and the reference electrode was mercury/mecurous sulphate (MMS). The latter was mounted in a side-arm filled with the working electrolyte but maintained at room temperature, separate from the cell, and connected to it via an electrolyte-filled glass tube tipped as a Luggin capillary. The reference electrode potential was calibrated to be 0.64 V(SHE). The counter electrode was placed at the end of the working cell opposite and facing the working electrode, and was provided with a porous separating partition to minimise mixing of the electrolyte surrounding it with the bulk working electrolyte. This is important since the counter electrode generates hydrogen when the working electrode is the anode, and transport of dissolved hydrogen to the anode could interfere with measurement of the methanol currents. The counter-electrode partition prevented this. The counter electrode compartment was equipped with a gas release vent as well, to allow evolved gases to escape. The entire cell was mounted in a fashion such that the counter electrode was up-hill relative to the working electrode in order to facilitate release of gases evolved at the counter electrode.

Both the single cell and the half cell were machined from polytetrafluoroethylene block. The cell carried a gas compartment to allow for feed of the reactive gas to the rear of the working electrode, i.e. the side facing away from the electrolyte; the working electrode thereby formed a membrane between the reactive gas and the electrolyte. The gas compartment was also machined from PTFE, with gas inlet and outlet facilities. In some experiments an end plate made of polymethylmethacrylate (Perspex) was used instead of PTFE in order to assess the possibility of electrolyte leakage; polymethylmethacrylate is transparent. In both cell arrangements, the electrodes were pressed against a current collector made of niobium sheet; sealing of the system was accomplished using gaskets made of Viton and expanded polypropylene. The current collector and gaskets were cut and shaped to fit the cell. The exposed working electrode was of circular geometry, diameter 2 cm, with an area of 3.14 cm^2. The collection of modules required for the completed cell was assembled using four long bolts made from 316L grade stainless steel, via machined holes which passed through the corners of the entire assembly.

For methanol oxidation studies, methanol vapour was provided from a vessel contained in a water bath at ca. 80 °C. In some experiments, argon was used as a carrier gas for the methanol; however, it was found that this decreased the performance at higher temperatures and higher flow rates. Some experiments were also carried out using a liquid methanol feed (5 M methanol in 1.5 M H_2SO_4); in this case, the fuel was fed to the cell via a second gas-lift pump. All methanol used was of analytical grade.

Experiments were also carried out with a complete single fuel cell, equipped for feeding fuel to the anode and oxygen or air to the cathode. The single cell is illustrated schematically in Fig. 1. The design employed for the single cell was similar to that of the half cell, except that the end carrying the counter electrode in the half cell was equipped for another gas-reactive electrode. The electrolyte was again heated externally and the single cell employed the same methanol feed system as described earlier. Unfortunately, the incorporation of the electrolyte inlet/outlet tubing and the thermistor require a rather large interelectrode separation, either 1.1 or 0.6 cm; this separation contributes significantly to the ohmic potential drop across the cell at high currents.

In all experiments, the polarisation characteristics were measured using a Solartron 1286 potentiostat in conjunction with a Hewlett-Packard microcomputer. Measurement of the ohmic potential drop was performed using a

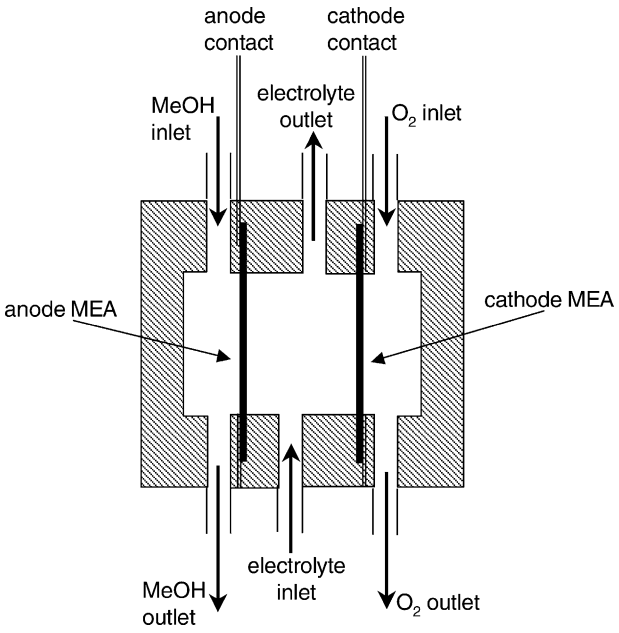

Fig. 1. Schematic diagram of a single cell (not to scale). Methanol is fed as a vapour into the fuel compartment. The electrolyte is circulated via a gas-lift pump (not shown) to maintain the temperature. The temperature is monitored via the thermistor (not shown) and used to control a heating element on the electrolyte pump. MEA stands for membrane electrode assembly, comprising the metallised porous polymer with the attached electrocatalyst layer. The shaded components were made from PTFE.

Hewlett-Packard 3314A function generator in conjunction with an IQ Tech ADC488/8SA analogue-to-digital converter. Experiments were carried out with the working cell at a temperature of between 59 and 75 °C, with most measurements being made at 70 or 75 °C, as tabulated below. In all the work presented, the electrode potential is expressed relative to the MMS reference electrode.

3. Results and discussion

In the course of the present work, several materials have been investigated for their suitability as both fuel and oxidant electrode substrates. All these materials were obtained from commercial suppliers, and descriptive details are summarised in Table 2. In order for a material to be suitable as an electrode substrate or membrane, it must be stable against attack from the strongly acidic electrolyte, as well as from ethandiol, Nafion and methanol. Moreover, such resistance to chemical attack must be maintained at the experimental cell operating temperature. Stability towards methanol is particularly important on the anode side, although possible cross-over of methanol means that it may also be important for the cathode side. In addition, the substrate must be stable towards processing temperatures up to the binding temperature used to make the electrode (120 °C). Of the materials tested, all were found to be suitably stable, with the exception of the Daramic membrane which reacted with methanol to give produce an oily residue. The identity of this oily residue was not determined.

In the case of the Tyvek L-1073D membrane (a spun-bonded polyethylene), a split membrane was made. This was produced in the form of two thinner membranes compressed together. The membrane was split into its two component parts by simply tearing the two halves apart; this procedure appeared to give the optimum membrane for the oxygen electrode (see results below).

According to the porosity and wetting characteristics of the various substrates, polymer or carbon, two electrode arrangements were adopted. If the substrate retained electrolyte then the catalyst layer was arranged facing the vapour chamber, and the non-catalyst side facing the working electrolyte. In this case, the electrolyte must permeate

Table 2
Details of substrate materials

Name/type	Supplier	Material	Thickness (μm)	Porosity (%)	Pore size (μm)
Daramic	W.R. Grace	Polyethylene	120	63	<0.1 (55%), 0.1–0.5 (39%)
Tyvek	DuPont	Spun-bound polyethylene			
L-1025D			135	–	–
L-1057D			150	31	–
L-1058D			155	25	–
L-1073D			186	40	–
L-1073B			183	21	–
L-1082D			255	35	–
L-1443R			130	–	–
L-1473R			215	–	–
Carbon paper	Torey	Carbon			
TGP-H-90			260	75.5	
TGP-H-60			119	77.4	
Durapore	Millipore	PTFE	–	–	5 (mean)
Jungfer	Lewis Industrial Products	PVC	250	34.9 (minimum) 35.4 (maximum) 35.2 (mean)	18 (minimum) 24 (maximum) 21 (mean)

PTFE: polytetrafluoroethylene. PVC: polyvinylchloride. Unknown data are marked with a dash.

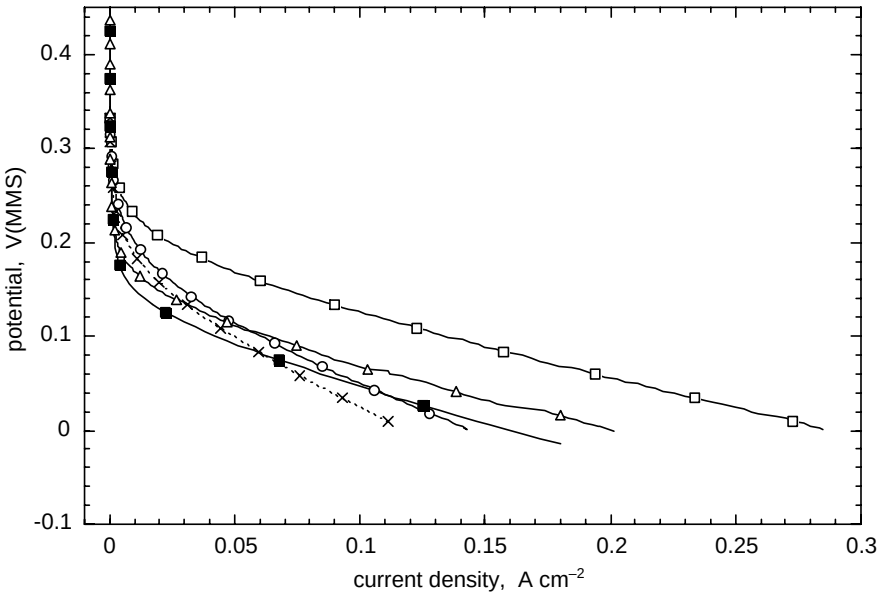

Fig. 2. Oxygen reduction polarisation curves for platinum electrodes prepared on various substrates: (□) electrode no. 14, oxygen; (×) electrode no. 14, air; (△) electrode no. 8, oxygen; (■) electrode no. 5, oxygen; (○) electrode no. 17, oxygen. See Table 3 for key to the electrodes.

the membrane and reach the catalyst layer. Alternatively, hydrophobic materials were arranged with the catalyst layer facing into the electrolyte. In this case the electrochemically reactive vapour (methanol for the anode, or oxygen or air for the cathode) must pass through the membrane in order to reach the catalyst.

3.1. Oxygen and air electrodes

The effectiveness of the various materials as cathode substrates for oxygen and air is shown in Fig. 2 and Table 3. From the polarisation curves in Fig. 2, it appears that the oxygen reduction reaction is subject to high activation

Table 3
Summary of results from the oxygen reduction half cell

No.	Substrate	Loading (mg Pt/cm^2)	i at 0 V(MMS) (mA/cm^2)		T (°C)	[H_2SO_4] (mol/dm^3)	Ink
			O_2	Air			
1	Daramic	0.03	10		70	1.5	1
2	Daramic	0.11	20		70	1.5	1
3	Daramic	0.13	37		70	1.5	1
4	Daramic	0.17	48		70	1.5	1
5	Daramic	0.31	85		70	1.5	1
			160[a]	94[a]			
6	L-1056K	0.08	88		70	3	1
7	L-1056K	0.17	135		70	3	1
8	L-1056K	0.37	201	81	70	3	1
9	L-1056K	0.11	30		70	3	6
10	L-1056K	0.27	165	41	70	3	6
11	L-1056K	0.35	136		70	3	6
12	L-1073D[b]	0.68	219		70	1.5	3
13	L-1073D[b]	0.89	250	135	70	1.5	3
14	L-1073D[b]	0.88	280	118	75	3	3
15	L-1073D[b]	1.90	250		70	1.5	3
16	L-1025D	1.16	200		75	3	3
17	Durapore	0.45	145		70	1.5	1

The left-hand column is the cathode number. The right-hand column refers to the ink number from Table 1. The substrates are detailed in Table 2. Substrates 6–16 are all Tyvek.

[a] Back pressure (0.07–0.14 atm).

[b] Membrane spilt in two.

polarisation limitations. The thermodynamic equilibrium electrode potential for the oxygen electrode reaction is ca. 0.59 V(MMS) (at 25 °C); however, very little current is detectable down to 0.25 V(MMS), a cathodic overpotential of 0.34 V. This is a direct consequence of the complex mechanism of oxygen reduction, a problem which has been the focus of extensive investigations [7,16–19]. At higher cathodic overpotentials, the polarisation characteristic becomes linear in nature indicating a fairly high ohmically resistive component. The ohmic resistance between the reference electrode and the working electrode was measured by current interruption to be ca. 0.28 Ω (0.88 Ω cm^2). Despite the polarisation loss mechanisms described earlier, there was no limiting current, and no evidence of the current even tapering towards one, regardless of the magnitude of the overpotential within the measured range.

With respect to both absolute performance and catalyst utilisation, electrodes based on the Tyvek membrane (spun-bonded polyethylene) appear to be the most effective. However, owing to the hydrophobic nature of this membrane material, these electrodes would only work with the catalyst layer facing into the electrolyte. In addition, a very small back pressure was required to force oxygen through the membrane to the catalyst–electrolyte interface. In the case of the Daramic membrane, the opposite was true. This substrate was found to be readily wetted and was arranged with the catalyst facing the reactive gas. This time, a slightly higher back pressure (ca. 0.07–0.14 bar) was required in order to create a good three-phase interface. These back pressures are far too small to regard the cell as being pressurised.

The effect of catalyst loading on the oxygen reduction reaction using electrodes based on Daramic, Tyvek and Durapore is shown in Fig. 3(a) and (b), summarised in Table 3. In Fig. 3(a), we show the current density as a function of the platinum loading. The catalyst utilisation is defined as the current generated per unit mass of catalyst; this is plotted in Fig. 3(b), and is achieved by dividing the current density

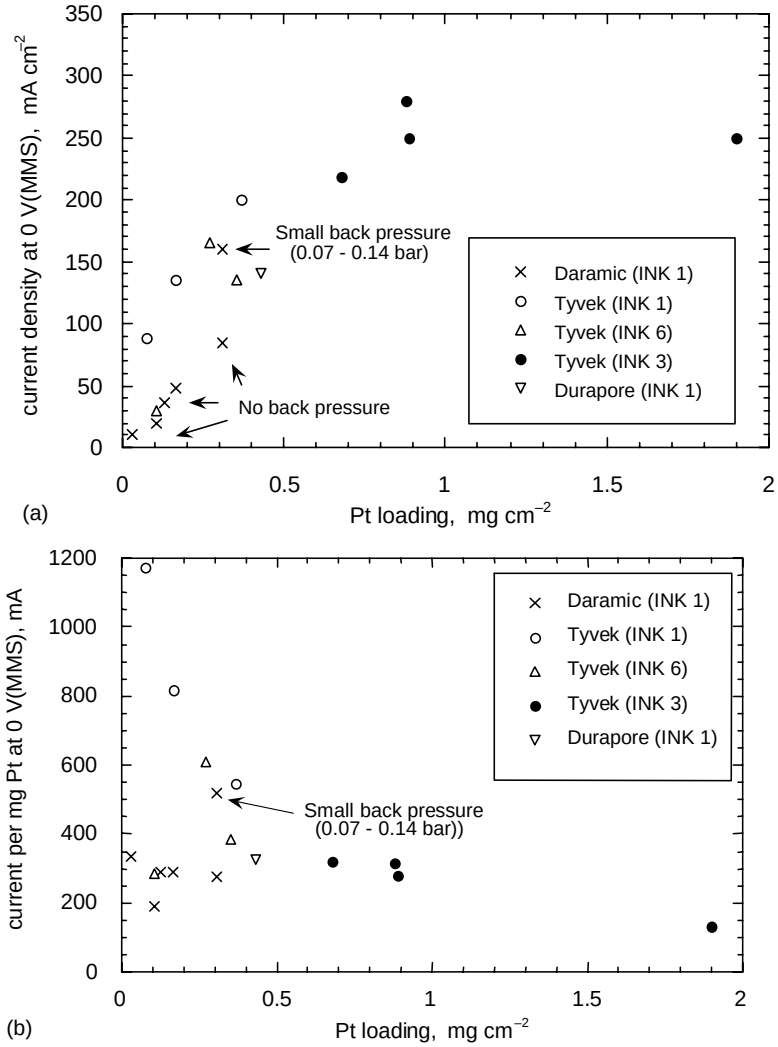

Fig. 3. Effect of platinum loading on steady state oxygen reduction current. (a) Current density measured at 0 V(MMS) (0.64 V(SHE)). (b) Same as (a), but given as the current adjusted to correspond to an electrode containing 1 mg platinum.

by the loading, shown in Fig. 3(a). In the cases which use ink no. 1, the form which contains platinum supported on carbon as the only platinum catalyst, the catalyst utilisation is approximately independent of the loading (Fig. 3(b)). However, the Tyvek electrode which uses ink no. 1 shows increasing platinum utilisation as the loading decreases, demonstrating that thickening the catalyst layer on this electrode does not improve the performance. One possible explanation for this effect is that the reaction interface between the catalyst, electrolyte and the fuel most probably tends to occur only at one region within the electrode, regardless of the loading. Increasing the loading (which would increase the thickness of the catalyst layer) would thus have no further effect and could serve only to increase the ohmic losses of the electrode.

In an attempt to increase the catalyst utilisation in the depth of the catalyst layer, a small amount of PTFE was incorporated together with the Nafion binder to help formation of gas channels within the entire depth of the electrode and thus increase the gas–electrolyte–catalyst interface. The composition determined by the Nafion-to-PTFE ratio was chosen from the work of Uchida et al. [20], who determined the best composition for use in a polymer electrolyte fuel cell. Although PTFE does not cure until much higher temperatures (ca. 360 °C), it was nevertheless hoped that, even at the lower curing temperatures used here, it might cross-link with the Nafion, as observed by Uchida et al. [20], and cause a stable structure to form. The result is shown as that for ink no. 6 in Fig. 3. These electrodes showed good structural properties, but no beneficial effect on the electrode performance was observed by adopting this procedure. By incorporating PTFE into the structure, other factors may well affect performance adversely, negating possible benefits from the procedure. For example, incorporated PTFE could increase the electronic resistance of the electrode by reducing contact between catalyst particles. Alternatively, the PTFE may coat some of the catalyst particles within the electrode structure, rendering those parts catalytically inactive or detached from neighbouring particles. It could also provide a more tortuous ion conduction route through the Nafion binder.

In accordance with these results, an attempt was made to increase the catalyst loading without increasing the electrode thickness. This was done by incorporating platinum black into the catalyst layer. In this way, loadings of around 1–3 mg Pt/cm^2 were possible within a reasonably thin electrode layer. Although not in direct proportion to the increased loading, a reasonable increase in performance was indeed observed, with the optimum loading being around 1 mg Pt/cm^2. In addition, the results obtained on air appear promising (Fig. 2 and Table 3). We also report our observation that, when air was used as the feed gas (rather than pure oxygen), the optimum current was found at high flow rates of the gas. This is likely to be associated with the nitrogen blanketing effect [21], in which nitrogen can accumulate over the catalyst after the oxygen component has reacted (see Fig. 2 and Table 3).

3.2. Methanol electrodes

Methanol electrodes were prepared using a variety of substrate materials and their performance is summarised in Figs. 4 and 5 and Table 4. As is the case for the cathodic oxygen reaction described above, the polarisation curves (Fig. 4) show a high degree of activation polarisation. This occurs as a direct consequence of the complex mechanism of methanol oxidation and its associated intermediates [12,21–27]. At higher anodic overpotentials, the polarisation characteristic

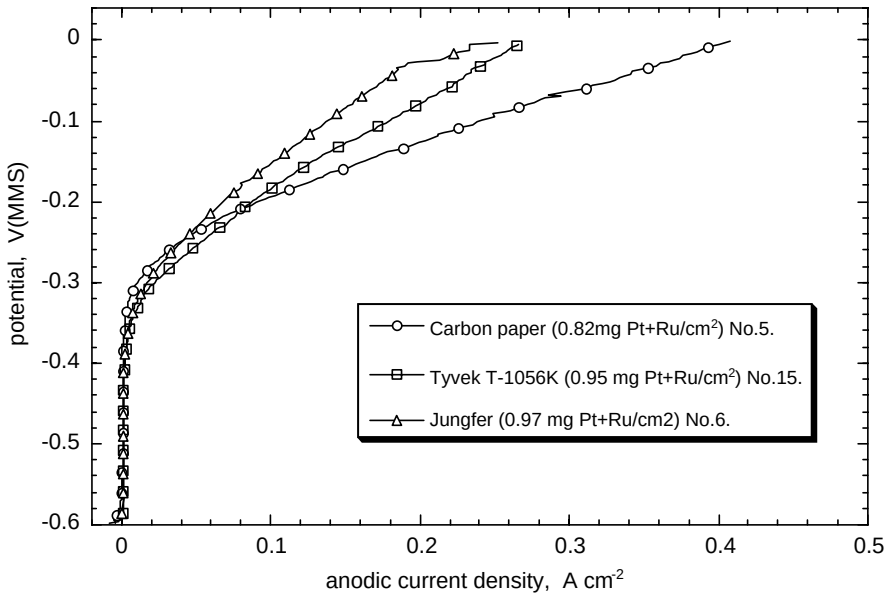

Fig. 4. Methanol oxidation polarisation curves for platinum/ruthenium electrodes prepared on various substrates: (○) electrode no. 5; (□) electrode no. 15; (△) electrode no. 6. See Table 4 for key to the electrodes.

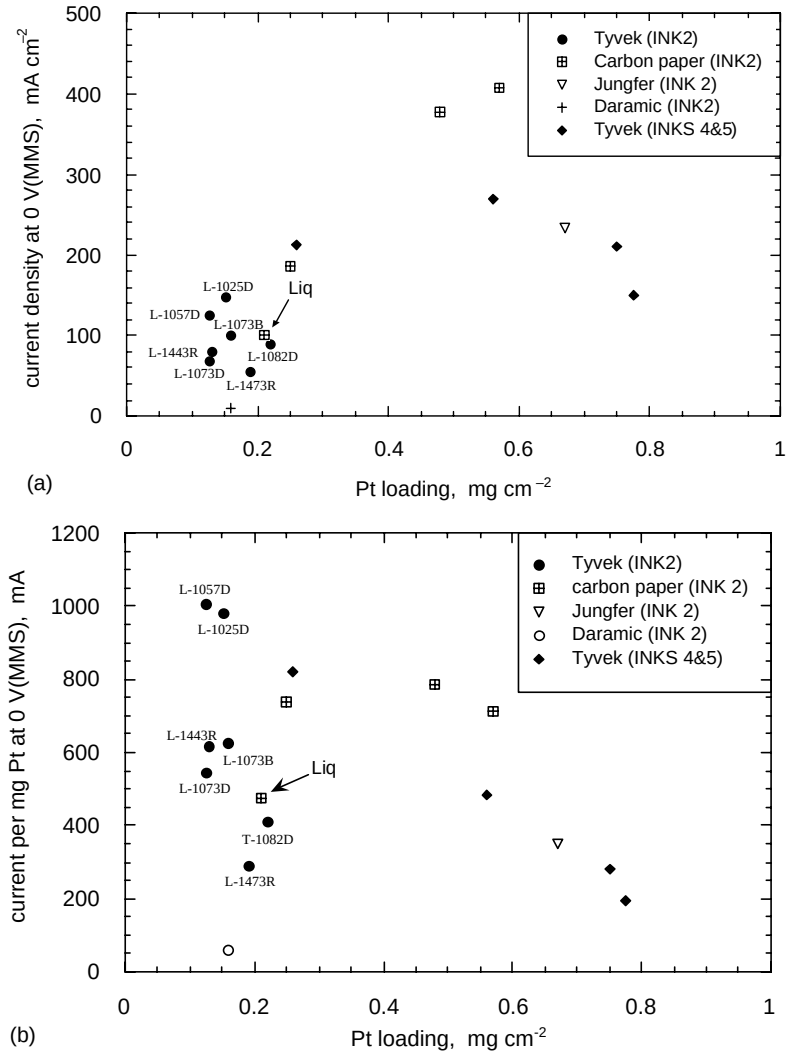

Fig. 5. Effect of platinum loading on steady methanol oxidation current. Liq refers to liquid methanol feed. All others are vapour methanol feed. (a) Current density measured at 0 V(MMS) (0.64 V(SHE)). (b) Same as (a), but given as the current adjusted to correspond to an electrode of 1 mg platinum.

becomes linear in nature indicating a significant resistive component.

With regard to overall performance, electrodes prepared using carbon paper show the highest methanol oxidation currents. The relative performance as a function of catalyst loading is shown in Fig. 5(a) in terms of current density, and in Fig. 5(b) in terms of catalyst utilisation. In preparing these electrodes, catalyst ink was observed to permeate into the interior of the carbon fibre structure, giving a greater distribution of the catalyst and possibly a higher catalyst utilisation. This lies in contrast to the Tyvek and the Daramic substrates, in which the catalyst remained essentially on the membrane surface. There is a general tendency in this case of achieving higher platinum utilisation towards lower catalyst loading (see Fig. 5(b)).

One important observation regarding the performance of the carbon-supported electrodes occurred at the methanol boiling temperature (65 °C), when a distinct change in performance occurred. Below the boiling point, the porous electrode appeared impermeable to the H_2SO_4 electrolyte and no back pressure was required to stop excessive leakage into the methanol vapour chamber. Above the boiling point, however, electrolyte was observed to leak excessively into the gas compartment, and a slight back pressure was required to stabilise the interface. Although this required careful attention to the operation of the cell, these changes were also accompanied by a significant increase in performance. In view of these results, it appears most likely that the adsorption of methanol on the catalyst surface, or the dissolution of methanol in the electrolyte, changes the interfacial energy of the system and the subsequent electrode filling level may shift to form a greater interfacial reaction zone.

As was observed for the case of the oxygen electrode, methanol electrodes based on Tyvek worked only with the catalyst layer facing the electrolyte. Although the substrate appears fully permeable to oxygen, the transport of methanol through the membrane seems to be difficult. As a result the performance was observed to be a little less favourable than

Table 4
Summary of results from the methanol oxidation half cell

No.	Substrate	Loading (mg/cm^2)		i at 0 V (MMS) (mA/cm^2)	T (°C)	[H_2SO_4] (mol/dm^3)	Feed type	Ink
		Pt + Ru	Pt					
1	Daramic	0.23	0.16	10	59	1.5	l	2
2	Carbon paper	0.30	0.21	100	59	1.5	l	2
3	Carbon paper	0.36	0.25	185	70	1.5	v	2
4	Carbon paper	0.69	0.48	377	70	1.5	v	2
5	Carbon paper	0.82	0.57	407	70	1.5	v	2
6	Jungfer	0.97	0.67	233	70	1.5	v	2
7	L-1082D	0.31	0.21	90	70	3	v	2
8	L-1073B	0.23	0.16	100	71	3	v	2
9	L-1073D	0.18	0.12	68	75	3	v	2
10	L-1057D	0.18	0.12	126	75	3	v	2
11	L-1025D	0.22	0.15	148	69	3	v	2
12	L-1473R	0.28	0.19	55	75	1	v	2
13	L-1443R	0.19	0.13	80	65	1.5	v	2
14	L-1056K	0.44	0.26	213	72	1.5	v	4
15	L-1056K	0.95	0.56	266	75	1.5	v	4
16	L-1056K	1.40	0.75	211	75	1.5	v	5
17	L-1056K	1.55	0.78	150	75	1.5	v	5

l: Liquid feed; v: vapour feed. The left-hand column is the anode number. The right-hand column is the ink number (see Table 1). The substrates are detailed in Table 2. Substrates 7–17 are all Tyvek. The ruthenium content of each electrode can be derived by subtracting the Pt content from the Pt + Ru content.

had been expected. Furthermore, the relative performance varies significantly with the thickness and type of Tyvek used. Since the best results occurred at the lowest loadings (i.e. for the thinnest catalyst layers), the loading was increased by incorporating the unsupported Adams Pt/Ru. In this way, higher loadings were achieved with a relatively thin catalyst layer. Again, as was the case with cathodes carrying added platinum black, the performance appears to be increased by the presence of the Adams Pt/Ru catalyst, but the improvement is still not in direct relation to the catalyst loading; this is seen in Fig. 5.

3.3. Results from the single cell

Single-cell results were obtained for a variety of electrode systems and are summarised in Figs. 6–8 and Table 5. In general, the results tend to reflect those expected from the respective half-cell measurements. Whereas cells incorporating anodes based on carbon paper appear to give the best performance with respect to power density (Fig. 7), they do so at the expense poor physical stability, with control necessary for electrolyte leakage into the gas compartment. In the case of the cells based on Tyvek, the

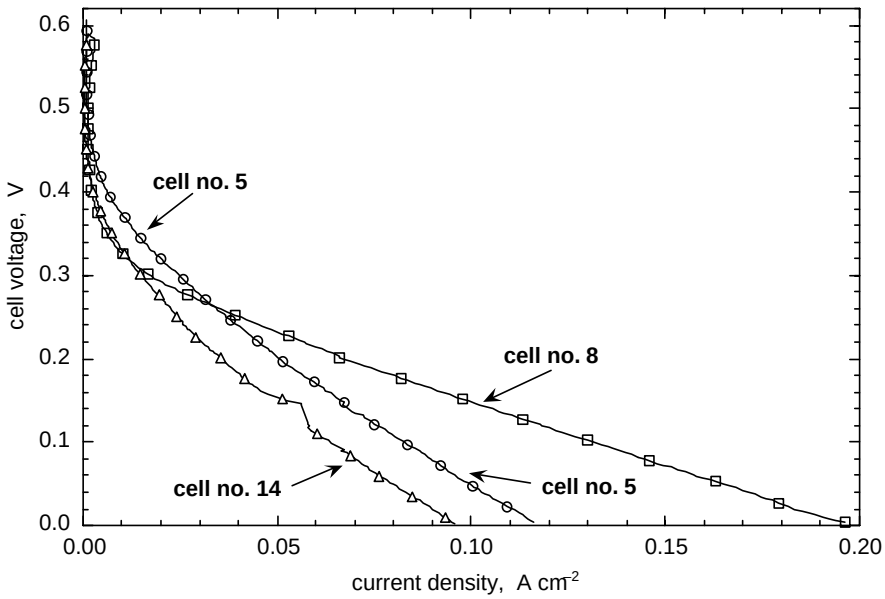

Fig. 6. Single-cell polarisation curves for various electrode assemblies: (□) cell no. 8; (○) cell no. 5; (△) cell no. 14. See Table 5 for key to the anodes and cathodes used in each cell.

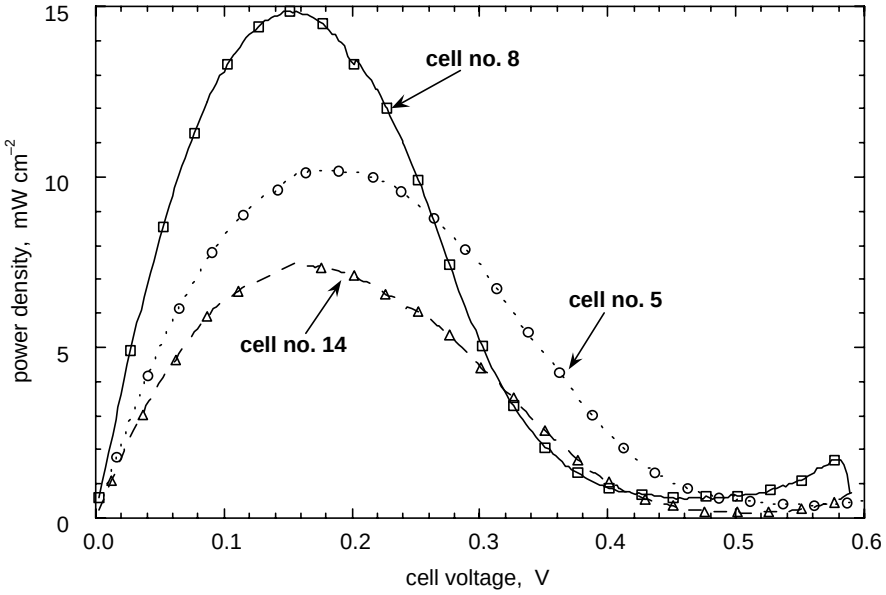

Fig. 7. Power density as a function of single-cell voltage for the DMFC using various electrode assemblies: (□) cell no. 8; (○) cell no. 5; (△) cell no. 14. See Table 5 for key to each cell.

opposite was true. The Tyvek-based cells gave consistently the maximum power per unit mass of platinum (see Fig. 8 and Table 5), with a maximum of 32.3 W/g Pt. In addition to a much higher utilisation of the platinum catalyst (Fig. 8), these electrodes were completely leak-proof. This spun-bonded polyethylene thus forms the most promising porous polymer so far investigated for the purpose of making such membrane electrodes. As described above, these electrodes were orientated with the catalyst facing into the electrolyte with the membrane acting as a hydrophobic backing, through which the reactive vapour must pass.

The results obtained here for the single methanol/oxygen cell still appear quite low in comparison with those achieved by other researchers. This can be ascribed largely to the more extreme operating conditions of the alternative cells. For example, in a paper by Ren et al. [1], it can be seen that a decrease in temperature from 130 to 70 °C corresponds to an approximate 10-fold decrease in current (measured at 0.5 V cell voltage and a pressure of 5 bar). The present system has been tested at temperatures up to 75 °C only, and ambient pressure through out.

Examination of the polarisation characteristics in Fig. 9 gives a good indication of the performance loss mechanisms

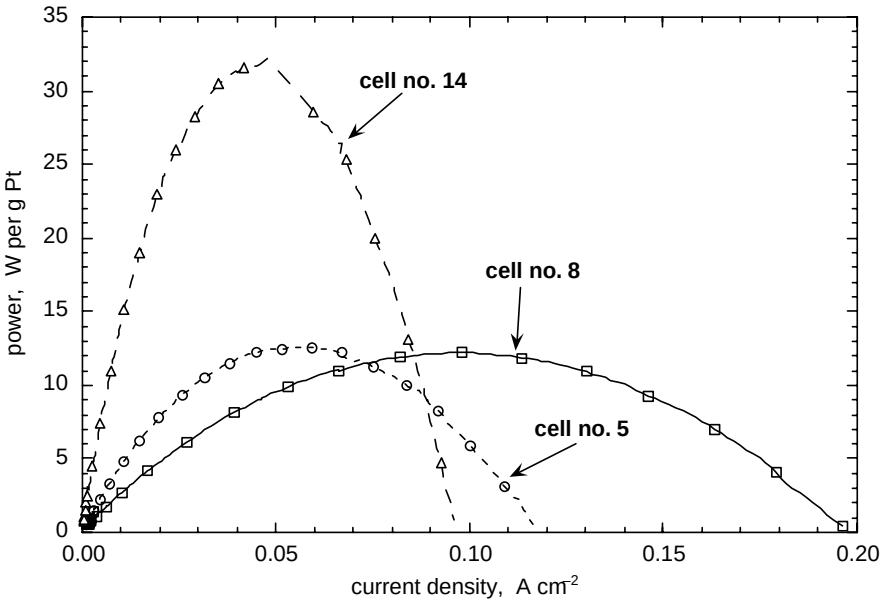

Fig. 8. Platinum utilisation curves for the DMFCs shown in Figs. 6 and 7: (□) cell no. 8; (○) cell no. 5; (△) cell no. 14. See Table 5 for the key to each cell.

Table 5
Summary of results from the full methanol/oxygen fuel cell

Cell no.	Anode	Anode loading (mg/cm^2)		Cathode	Cathode loading (mg Pt/cm^2)	Gap (cm)	T (°C)	Maximum current density (mA/cm^2)	Maximum power density (mW/cm^2)	Maximum power (W/g Pt)
		Pt + Ru	Pt							
1	Carbon paper	0.66	0.46	Daramic	0.34	1.1	70	80	–	–
2	Carbon paper	0.90	0.62	Carbon paper	0.64	1.1	70	110	9.3	7.4
3	Carbon paper	0.86	0.60	Daramic	0.38	1.1	70	105	9.0	9.2
4	Carbon paper	0.71	0.49	Daramic	0.44	1.1	70	105	9.0	9.6
5	Carbon paper	1.13	0.78	Daramic	0.44	1.1	70	116	10.7	8.8
6	Carbon paper	0.76	0.53	Daramic	0.31	0.6	73	96	7.7	9.2
7	Carbon paper	0.98	0.68	Daramic	0.28	0.6	70	109	9.3	9.7
8	Carbon paper	0.95	0.66	T-1056K	0.15	0.6	75	196	15.6	19.2
9	Carbon paper	0.90	0.62	T-1056K	0.33	0.6	75	140	–	–
10	T-1056K	0.15	0.10	T-1056K	0.15	0.6	75	–	6.5	25.6
11	L-1057D	0.34	0.23	T-1056K	0.20	0.6	75	105	8.0	18.6
12	Carbon paper	0.80	0.56	T-1056K	0.20	0.6	75	–	12.3	16.2
13	Jungfer	0.75	0.52	T-1056K	0.20	0.6	75	–	6.1	8.5
14	T-1056K	0.23	0.16	T-1056K	0.07	0.6	75	100	7.5	32.3

"Gap" refers to the interelectrode spacing. The substrates are detailed in Table 2.

involved. At low current densities, the system appears governed by a high degree of activation polarisation as expected from the half-cell results. At higher overpotentials, the polarisation is linear in current, indicating a limitingly high ohmic resistance. This is expected, considering the large interelectrode gap adopted for the single cell, necessary in order to allow the simple system to be measured and controlled. The high resistive losses are further illustrated by looking at the polarisation curves corrected for the ohmic potential drop in Fig. 9. The ohmic-drop-corrected data in Fig. 9 were calculated from the measured ohmic resistance, which was found to be $0.28 \pm 0.03\,\Omega$ ($0.88\,\Omega\,cm^2$) for the cathode and $0.26 \pm 0.01\,\Omega$ ($0.82\,\Omega\,cm^2$) for the anode. Although some fraction of these ohmic corrections must be associated with the electronic resistance within the electrode structure, which is always present, it is apparent that reducing the interelectrode gap should reduce the ohmic resistance considerably.

Some loss of performance from the single cell may also be expected from methanol cross-over. The effect is probably the cause of the relatively low open-circuit cell voltage of 0.6 V shown in Fig. 7. Half-cell experiments as shown in Fig. 9 indicate that the open-circuit single-cell voltage should be around 0.9 V. The difference between these may well be a consequence of methanol cross-over from anode to cathode. Although not measured, some methanol must diffuse across and decrease the cathode performance, despite the fact that the experiments were carried out above

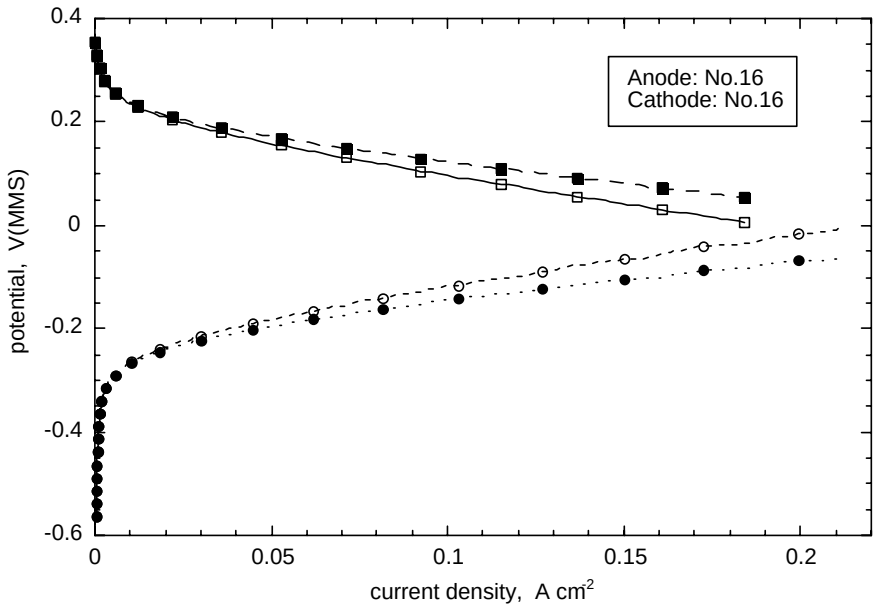

Fig. 9. Polarisation curves for oxygen cathode no. 16 (■, □; see Table 3) and methanol anode no. 16 (●, ○; see Table 4) plotted as raw data (□, ○) and also showing data corrected for the ohmic potential drop (■, ●). Data acquired using the half cells.

the methanol boiling temperature. Loss of cathode performance arises first from a parasitic anodic reaction at the cathode. Methanol oxidation at the cathode must also poison the cathode electrocatalyst because of intermediate components produced by the oxidised methanol, notably carbon monoxide. The cathode we used was pure platinum and notoriously susceptible to CO poisoning. It is not known how serious this effect is in comparison with that observed in the more conventional DMFC where a thin layer of proton exchange membrane serves as the electrolyte [4–9]. This would depend very much on the rate of methanol cross-over, which is yet to be measured. However, the use of sulphuric acid of high conductivity allows potentially a thicker layer of electrolyte to be employed.

Apart from the low cost of the components used in the sulphuric acid/porous polymer electrolyte membrane, one potential advantage of the liquid electrolyte over the proton exchange membrane is the potential ability to circulate the electrolyte, either continuously or intermittently. Circulating the electrolyte from a reservoir allows the electrolyte to be monitored and controlled during operation; the contents of the electrolyte can even be replaced if necessary. This would give good control of the potential build-up of impurities during longer-term operation which may degrade performance. It would also provide ready access to the control of the water content; water production at the cathode would dilute the electrolyte. Electrolyte circulation also allows management of any dissolved methanol.

4. Conclusions

Several microporous materials have been tested for their suitability as electrode substrates for use in a DMFC employing H_2SO_4 as electrolyte. Apart from the carbon paper, these were all low-cost commercially available polymers. With the exception of carbon paper, all were physically stable under the operating conditions of the cell. In the case of the carbon paper electrodes, a small pressure differential was required at higher temperatures to create a stable interface. All the membranes tested were chemically stable in the presence of H_2SO_4 at the temperatures of the experiments. However, the Daramic membrane appeared to release a component in the presence of methanol the identity of which is not known. Electrodes based on Tyvek, a spun-bonded polyethylene, showed high activity and platinum utilisation towards both methanol oxidation and oxygen reduction reactions. Unfortunately, increasing the platinum/ruthenium loadings did not give a corresponding linear increase in performance although the addition of unsupported catalysts (e.g. Adams platinum/ruthenium and platinum black) to the structure did show some improvement.

Application of the various electrode systems to a single cell proved successful and simple. Although the single-cell performances reported here are considerably lower than that required for automotive application, reduction of the inter-electrode gap in a more practical cell design together with possible pressurisation should increase the performance significantly. Further performance increase should also be possible by optimising both the catalyst/binder composition and the active catalyst preparation method.

Acknowledgements

We are grateful to the EPSRC for the financial support of this programme.

References

[1] X. Ren, M.S. Wilson, S. Gottesfeld, J. Electrochem. Soc. 143 (1996) L12.
[2] A.K. Shukla, P.A. Christensen, A. Hamnett, M.P. Hogarth, J. Power Sources 55 (1995) 87.
[3] J.-T. Wang, S. Wasmus, R.F. Savinell, J. Electrochem. Soc. 143 (1996) 1223.
[4] A. Kuver, I. Vogel, W. Vielstich, J. Power Sources 52 (1994) 77.
[5] A. Kuver, I. Vogel, W. Vielstich, in: Proceedings of the 45th Annual Meeting of the International Society of Electrochemistry, Porto, Portugal, 28 August–2 September 1994 (Abstract OIV-4).
[6] A.S. Arico, V. Antonucci, V. Alderuccii, E. Modica, N. Giordano, J. Appl. Electrochem. 23 (1993) 1107.
[7] S.C. Thomas, X.M. Ren, S. Gottesfeld, P. Zelenay, Electrochim. Acta 47 (2002) 3741.
[8] Z.G. Shao, X. Wang, I.M. Hsing, J. Membr. Sci. 210 (2002) 147.
[9] B. Garau, E.S. Smotkin, J. Power Sources 112 (2002) 339.
[10] G.T. Burstein, A.R. Kucernak, C.J. Barnett, K.R. Williams, J. Appl. Electrochem. 27 (1997) 1304.
[11] D. Dobos, Electrochemical Data, Elsevier, Amsterdam, 1975, pp. 42–43.
[12] G.T. Burstein, C.J. Barnett, A.R. Kucernak, K.R. Williams, Catal. Today 38 (1997) 425.
[13] C.J. Barnett, G.T. Burstein, A.R. Kucernak, K.R. Williams, Electrochim. Acta 42 (1997) 2381.
[14] D.R. McIntyre, G.T. Burstein, A Vossen, J. Power Sources 107 (2002) 67.
[15] D.R. McIntyre, A. Vossen, J.R. Wilde, G.T. Burstein, J. Power Sources 108 (2002) 1.
[16] J.D.E. McIntyre, D.E. Aspnes, Bull. Am. Phys. Soc. 15 (1970) 366.
[17] S. Gottesfeld, I.D. Raistrick, S. Srinivasan, J. Electrochem. Soc. 134 (1987) 1455.
[18] D.R. Lawson, L.D. Whiteley, C.R. Martin, M.N. Szentirmay, J.I. Song, J. Electrochem. Soc. 135 (1988) 2247.
[19] A. Parthasarathy, B. Dave, S. Srinivasan, A.J. Appleby, C.R. Martin, J. Electrochem. Soc. 139 (1992) 1634.
[20] M. Uchida, Y. Aoyama, N. Eda, A. Ohta, J. Electrochem. Soc. 142 (1995) 4143.
[21] K.R. Williams (Ed.), An Introduction to Fuel Cells, Elsevier, Amsterdam, 1966, pp 97 et seq.
[22] V.S. Bagotzky, Y.B. Vassiliev, O.A. Khazova, J. Electroanal. Chem. 81 (1977) 229.
[23] R. Nichols, A. Bewick, Electrochim. Acta 33 (1988) 1691.
[24] R. Parsons, T. VanderNoot, J. Electroanal. Chem. 257 (1988) 9.
[25] T. Iwasita, F.C. Nart, J. Electroanal. Chem. 317 (1991) 291.
[26] T. Iwasita, F.C. Nart, B. Lopez, W. Vielstich, Electrochim. Acta 37 (1992) 2361.
[27] J. Munk, P.A. Christensen, A. Hamnett, E. Skou, J. Electroanal. Chem. 401 (1996) 215.